Anisotropic kinetics of vacancy diffusion and annihilation on Si(001) surfaces studied by scanning reflection electron microscopy

Heiji Watanabe and Masakazu Ichikawa
Joint Research Center for Atom Technology, Angstrom Technology Partnership,
c/o National Institute for Advanced Interdisciplinary Research, 1-1-4 Higashi, Tsukuba, Ibaraki 305, Japan
(Received 1 July 1996)

The kinetics of vacancy diffusion and annihilation on Si(001)-2×1 surfaces are studied by using scanning reflection electron microscopy. The S_B steps, which run across dimer rows, retreat 1.8 times faster than S_A steps during low-energy Ar-ion sputtering at elevated substrate temperatures. This leads to virtual single-domain stabilization in the initial stage of layer-by-layer sputtering. These different types of steps maintain an equilibrium configuration due to a step-step interaction. On wide terraces, elongated vacancy islands with a single atomic height and alternative 2×1 reconstruction are formed along the dimer rows. These results indicate preferential vacancy annihilation at S_B steps and anisotropic vacancy diffusion depending on the dimer row direction. The diffusion length of the vacancies is estimated from the width of the denuded zones of the vacancy islands, which are formed on both sides of the atomic steps by thermal heating after vacancy introduction at room substrate temperature. The activation energy for vacancy diffusion along the dimer rows is obtained to be 2.3±0.2 eV. A vacancy diffusion model mediated by dimer vacancy complexes rather than single-dimer vacancies, interprets our experimental results. [S0163-1829(97)00315-9]

I. INTRODUCTION

The kinetics of adatom diffusion have been extensively studied by using many kinds of surface analyses, especially for Si surfaces. This is because of its technological importance in thin-film growth and because of scientific interest. Compared to Si(111) surfaces, which show large-scale surface reconstruction with a 7×7 period and isotropic behavior for adatom diffusion, it is well known that a Si(001) surface involving 2×1 reconstruction is anisotropic and shows unique behavior.[1–8] For example, the diffusion barrier of surface adatoms along the dimer rows is much smaller than that in the crossing direction.[2,3] Also, various kinds of surface reconstructions, such as $c(2\times4)$ and $2\times n$ structures, have been reported, depending on preparation conditions,[4–6] and there are straight and wavy steps called S_A and S_B steps, which run parallel and perpendicular to the dimer rows on the upper terraces.[7] The different nature of these steps results in preferential adatom sticking and in the formation of a virtual single-domain surface during homoepitaxial growth.[8]

In addition, because many intrinsic dimer vacancies have been observed by scanning tunneling microscopy (STM) for Si(001) surfaces,[1,9] several experimental and theoretical studies have been performed to clarify the vacancies in recent years.[6,10–19] Bedrossian *et al.* reported reflection high-energy electron diffraction (RHEED) intensity oscillation during low-energy Xe-ion sputtering at an elevated substrate temperature; this suggested layer-by-layer removal of Si atoms from Si(001) surfaces.[10,11] They also observed the relative motion between the S_A and S_B steps during sputtering and reported single-domain stabilization.[12] To describe these unique phenomena, one should understand the diffusion kinetics of dimer vacancies, as well as their static nature. Previously, the motion of a single-dimer vacancy, as the most simple and basic process on Si(001) surfaces, was analyzed using a different application of STM by Kitamura, Legally, and Webb.[15]

Swartzentruber and Schacht also measured an effective activation barrier for rearrangement of wavy S_B steps.[14] However, because there has been relatively little work dealing with diffusion kinetics and because the anisotropy of Si(001) surfaces makes this issue complicated, the details are not yet well understood.

In previous works, we studied layer-by-layer atom removal from Si(111) surfaces during low-energy Ar-ion sputtering by using scanning reflection electron microscopy (SREM).[18] We also demonstrated the use of an alternative SREM technique to analyze vacancy diffusion.[19] The results showed that vacancy diffusion on this surface was isotropic and had an activation barrier of 3.0 ± 0.2 eV. This energy barrier was explained by using the potential barrier both for the surface diffusion of adatoms and for the lateral binding energy to release adatoms from steps.[19]

In this paper, we present a SREM study of vacancy diffusion and annihilation kinetics on Si(001)-2×1 surfaces. The motion of two kinds of atomic steps (S_A and S_B steps) is investigated by *in situ* SREM observation, in which alternating domains of 1×2 and 2×1 appear with different contrasts. The diffusion length of vacancies is estimated from the width of denuded zones of the vacancy islands, which are created along steps by thermal heating after vacancy introduction by low-energy ion impact. The kinetics of vacancy diffusion on Si(001) is discussed based on the experimentally obtained activation barrier and previous theoretical and experimental studies.

II. EXPERIMENT

We used an ultrahigh vacuum (UHV) surface analysis system,[20] which performs high-resolution SREM.[21] This sys-

 © 1997 The American Physical Society

tem is equipped with an UHV thermal field emission electron gun (modified Hitachi S-4200 scanning electron microscope) and an Ar-ion gun. The base pressure of the analysis chamber was 3×10^{-11} Torr. A 30-keV electron beam with a 3 nm diameter and a 0.2 nA current was used for UHV-SREM observation. The diffraction patterns were monitored on a fluorescent screen by a charge-coupled device camera (microprobe RHEED). The intensity of the diffraction spot used for the SREM image was detected by a photomultiplier through an optical lens and optical fiber. In this study, all SREM images were obtained by recording the changes in specular spot intensity. The bright and dark contrast terraces correspond to the 1×2 and 2×1 domains, respectively.

A Si(001) sample with dimensions of $11\times2.5\times0.45$ mm^3 was cut from a low-resistivity wafer and was first outgassed by using a pyrolytic graphite pyrolytic boron nitride (PG/PBN) ceramic heater at 550 °C for 12 h. Then, flash heating (at 1100 °C for 10 s) was performed by direct current at UHV conditions of less than 1.5×10^{-10} Torr. This procedure produces typical clean Si(001)-2×1 surfaces showing alternative 2×1 and 1×2 terraces. These 2×1 (A-domain) and 1×2 (B-domain) terraces have dimer rows that run parallel and perpendicular to the incident electron beam, respectively. Using the electromigration effect,[22] we can modify the ratio between A- and B-domain populations by changing the current direction during subsequent high-temperature annealing. An optical pyrometer was used to measure the substrate temperatures. During ceramic heating, sample temperatures were corrected by measuring the PG/PBN heater surface covered with graphite. To study vacancy kinetics, the samples were heated with the ceramic heater to avoid the electromigration effect.

After sample preparation, Ar ions with a 500-eV kinetic energy were irradiated onto the Si(001)-2×1 surface. The ion current and incident angle were 16 nA/cm^2 and 43° to the surface, respectively. The Ar-gas pressure in the analysis chamber was kept at 2×10^{-8} Torr during sputtering. For the first experiment, ion sputtering was performed at elevated substrate temperatures. The absolute motion of the atomic steps was analyzed after the sample was cooled to room temperature. For the second experiment, after vacancy introduction, the substrate was heated with a ceramic heater to measure the diffusion length of vacancies from the width of the denuded zones, which included few vacancy islands. The use of this technique has been reported by Doi *et al.* for evaluating adatom diffusion on Si(001) surfaces.[23]

During low-energy ion bombardment, collisions with the substrate are limited to a few atoms, so some of these atoms are ejected from the surface without displacing other atoms. In addition, ion bombardment at a high substrate temperature leads to the repair of the surface structure. This thermal repair was confirmed from the continuous RHEED intensity oscillation during low-energy ion sputtering[10] and STM images showing the 2×1 reconstruction on the ion-beam-irradiated Si(001) surfaces at a 400 °C substrate temperature.[12] In our experiments, the Ar-ion current density of 16 nA/cm^2 was much lower than that of the previous reports and the ion dose for vacancy introduction in Sec. III B was extremely small. In addition, our annealing temperatures were higher than those used in the previous STM study. For these reasons, the ion-beam-induced damage can be ignored

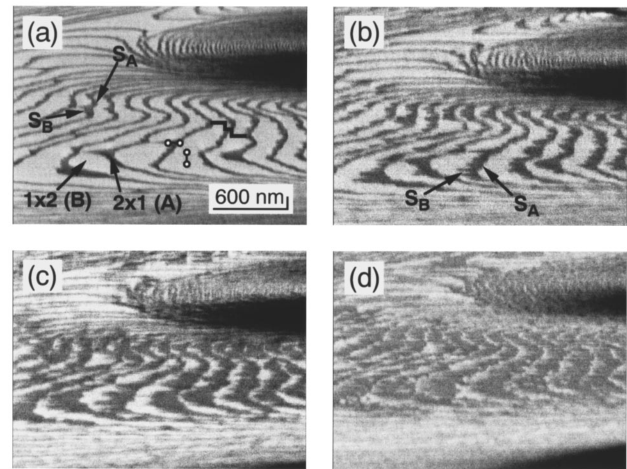

FIG. 1. SREM images of Si(001)-2×1 surfaces before and after low-energy Ar-ion sputtering. (a) The clean surface prepared by flash heating. The 2×1 (A-domain) and 1×2 (B-domain) terraces appear to have dark and bright contrast, respectively. This B-domain majority surface becomes lower from left to right. A protrusion with narrow terraces at the upper right portion is an edge of a large island formed by a SiC particle during sample preparation. (b)–(d) Results of 500-eV ion irradiation at a 689 °C substrate temperature with ion doses of 2.4×10^{14}, 4.8×10^{14}, and 7.2×10^{14} ions/cm^2, respectively. During ion sputtering, a typical 2×1 RHEED pattern was observed.

in our experiment. Even if a small amount of surface damage remains on the surface, the vacancy diffusion kinetics at the minority sites are likely to be thinly spread over the entire surface.

III. RESULTS AND DISCUSSIONS

A. Step motion and vacancy island formation

Figure 1(a) shows a SREM image of the Si(001)-2×1 surface prepared by flash heating. On this surface, the B domains with bright contrast form a majority and the surface becomes lower from left to right. The terraces are separated by straight S_A steps and rough S_B steps of a single atomic height. Since the SREM image is vertically compressed, these atomic steps wave gently. The protrusion with narrow terraces in the upper right portion is an edge of a large island formed by a SiC particle during sample preparation. Figures 1(b)–1(d) are the results of low-energy ion sputtering at a 689 °C substrate temperature with ion doses of 2.4×10^{14}, 4.8×10^{14}, and 7.2×10^{14} ions/cm^2, respectively. After ion sputtering, microprobe RHEED patterns revealed typical 2×1 and 1×2 reconstructions on the dark and bright terraces and the S_B steps retreated with respect to the straight S_A steps. This resulted in an increase of the A-domain population and the initial B-domain majority surface was reversed to an A-domain-stabilized surface [Fig. 1(d)]. These results indicate that vacancies created by low-energy ion impact are movable to the step edges, where they are annihilated. This process is characterized by a reversal of the step-flow mode for film growth. Moreover, selectivity of vacancy annihilation at S_B steps forms a virtual single-domain stabilized surface at the initial stage of layer-by-layer sputtering. This result is consistent with previous STM work.[12,13] At a low ion

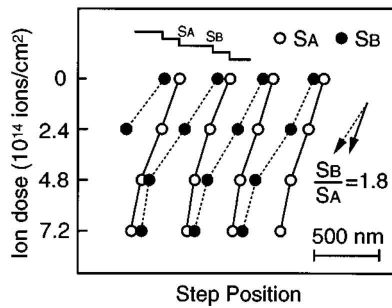

FIG. 2. Step motion during layer-by-layer sputtering measured from SREM images in Fig. 1. The position of each step is plotted as a function of ion dose. The open and filled circles show the motion of S_A and S_B steps, respectively. At the beginning of ion sputtering, S_B steps retreat 1.8 times faster than S_A steps.

dose of 2.4×10^{14} ions/cm^2 [Fig. 1(b)], the S_B steps become much rougher and the S_A steps remain straight. However, with an increased ion dose, the S_A steps also become rough. This is because a small amount of the S_B portion involved in the gently waving S_A steps acts as a sink for vacancy annihilation.

Compared to usual STM observations, large-scale SREM observation, which involves an object as a marker, informs us about absolute step motion. For example, since the large SiC island in Fig. 1 does not move in the initial stage of layer-by-layer sputtering, we can measure the absolute motion of individual steps as a function of ion dose. The change in the position of the step front measured from Fig. 1 is plotted in Fig. 2. The solid and dotted lines (open and filled circles) show the motion of S_A and S_B steps, respectively. At first, the S_B steps retreat 1.8 times faster than the S_A steps. This means that the probability of vacancy annihilation is 1.8 times larger at the S_B steps than at the S_A steps. Then, after the S_B steps catch up with the S_A steps, the speed of the S_B steps becomes equal to that of the S_A steps and these steps maintain a certain distance from each other of less than 100 nm. Because this equilibrium step configuration is determined by the balance of selective vacancy annihilation at S_B steps and thermal healing, ion sputtering at high temperature makes the distance between these steps longer than that of previous STM studies[12,13] due to increased thermal healing. [Note that since the speed of the S_B steps does not change within the ion dose of 4.8×10^{14} ions/cm^2 (Fig. 2), where the major B domain becomes a minority, the thermal healing effect cannot be the driving force for selective vacancy annihilation at the S_B steps.] Moreover, a slight decrease in motion of the S_A steps is also observed at an ion dose of over 4.8×10^{14} ions/cm^2. Considering anisotropic vacancy diffusion along the dimer rows, this result is attributed to the decrease in vacancy transport perpendicular to the steps on the 2×1 terraces. The details of anisotropy will be discussed later.

Next, we used an A-domain majority sample as an initial surface. The flash-cleaned Si(001) surface was annealed at 900 °C by using step-down current for 8 min. This formed a B-domain majority surface consisting of wide terraces and bunched steps. Then, the sample was heated again by using step-up current for 3 min to replace the wide B-domain terrace with an A-domain terrace [Fig. 3(a)]. Figure 3(b) shows

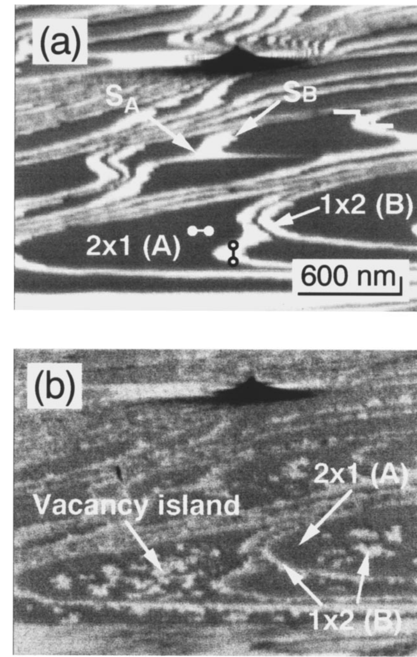

FIG. 3. SREM images of the A-domain majority Si(001) surface before and after ion irradiation at a 689 °C substrate temperature. (a) An initial surface, which consists of wide 2×1 terraces, prepared by high-temperature annealing at 900 °C using direct current. (b) The result of ion sputtering with a dose of 2.4×10^{14} ions/cm^2. The bright contrast islands on wide 2×1 terraces show clear 1×2 RHEED patterns.

the results of ion sputtering of this surface at the same substrate temperature (689 °C) and ion dose (2.4×10^{14} ions/cm^2) as in Fig. 1(b). In spite of the initially A-dominated surface, it is clear that the S_B steps retreat with respect to the S_A steps again and the surface maintains an equilibrium configuration with a step distance of less than 100 nm. These results correlate well with those of Figs. 1 and 2 and mean that the selective annihilation of vacancies at the S_B steps is intrinsically independent of the initial surface. The main feature of this figure is that vacancy islands, which show a 1×2 microprobe RHEED pattern, are formed on the wide 2×1 terraces. This result suggests that individual vacancies on the wide terraces cannot reach the step edges and they form vacancy islands with a single atomic height (two-dimensional island growth), as illustrated in Fig. 4. Considering the vertical compression of this SREM image, it is

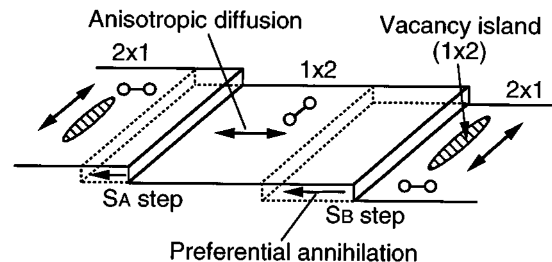

FIG. 4. Schematic illustration of vacancy diffusion and annihilation on Si(001) surfaces. The main features on the surface are elongated vacancy islands along the dimer rows and preferential S_B step retraction.

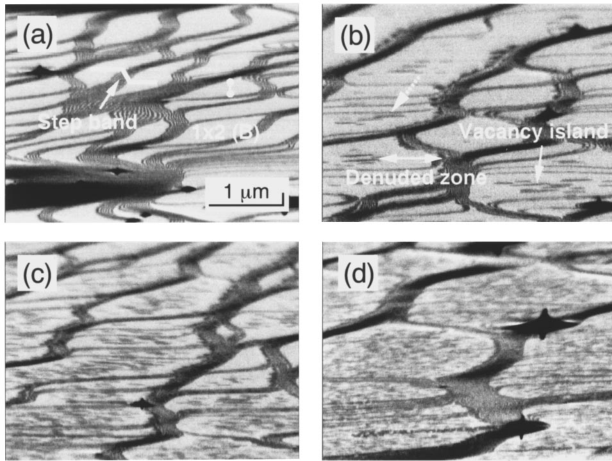

FIG. 5. Formation and diffusion of vacancy islands on Si(001)-2×1 surfaces. (a) An initial surface prepared by high-temperature annealing at 900 °C. This surface includes wide 1×2 terraces and bunched steps and becomes lower from left to right. After vacancy introduction onto this surface by low-energy ions at a dose of 1.4×10^{14} ions/cm^2, the sample was heated in a temperature range from 597 °C to 737 °C by using a ceramic heater. (b)–(d) Typical results of thermal heating at 737 °C for 10 min, 698 °C for 10 min, and 624 °C for 30 min, respectively. The dark portions on wide terraces correspond to vacancy islands, which are elongated along dimer rows. Denuded zones, which include no vacancy islands, are observed along the step band.

obvious that these vacancy islands are elongated along the dimer rows of the wide 2×1 terraces. Moreover, since step retraction observed for wide 1×2 terraces on the B-domain majority surface (Fig. 1) shows a sufficient vacancy mobility, we can conclude that vacancies diffuse anisotropically along the dimer rows. Note that denuded zones, which include few vacancy islands, are formed at the edges of wide 2×1 terraces.

B. Activation energy for vacancy diffusion along the dimer rows

When the sample was sputtered at elevated substrate temperatures, vacancy creation and diffusion occur simultaneously. Here we investigate the vacancy diffusion kinetics by analyzing the denuded zone width on the Si(001) surfaces formed by thermal heating after vacancy creation at room temperature. We prepared a B-domain (1×2 terrace) majority surface by high-temperature annealing at 900 °C by using step-down current. The SREM image of this initial surface is shown in Fig. 5(a), where wide 1×2 terraces and bunched steps are observed. Unfortunately, since the SREM image is vertically compressed and we used a highly oriented Si(001) wafer, the atomic steps on this surface wave gently and cannot be arranged exactly parallel to the incident electron beam. In this case, denuded zones created by vacancy diffusion along the dimer rows on 1×2 terraces are clearly observed.

Vacancies were introduced onto this surface by low-energy Ar-ion irradiation at a dose of 1.4×10^{14} ions/cm^2 at room substrate temperature. Then the sample was heated in the temperature range from 597 °C to 737 °C by using a PG/PBN heater in UHV conditions. Although a RHEED pattern from 1×2 reconstruction could hardly be observed after ion irradiation, clear 1×2 RHEED patterns appeared at the beginning of thermal heating. This suggests that ion-beam-induced structural damage was rapidly repaired. Therefore, we believe that vacancy diffusion during further thermal heating can be treated as a surface process on a Si(001)-2×1 surface. Figures 5(b)–5(d) show typical results of thermal heating at 737 °C for 10 min, 698 °C for 10 min, and 624 °C for 30 min, respectively. In these SREM images, we can recognize the formation of vacancy islands on the wide 1×2 terraces, as well as the creation of denuded zones. As shown in Fig. 5(b) high-temperature annealing allows long-range vacancy diffusion and forms large vacancy islands and wide denuded zones. Figure 6 is a magnified SREM image after thermal heating at 718 °C for 10 min and Fig. 7 illustrates the features of these surfaces. It is obvious that vacancy islands are elongated along dimer rows on the wide 1×2 terraces, the same as in Fig. 3. The upper S_B step of the step band in Fig. 6 selectively retreats and becomes rough due to vacancy annihilation. As a result, a 2×1 terrace is formed underneath the S_B step. The width of the denuded zone formed on the upper 1×2 terrace (W_B) is wider than that of the low side of the step band (W_A) because vacancy density becomes larger at the lower side than at the upper side due to the selective vacancy annihilation at the S_B step. In addition, contrary to the rough S_B step, the S_A step at the bottom of this step band remains smooth.

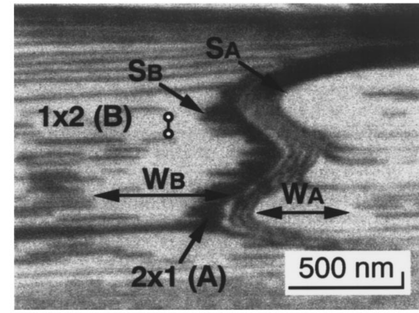

FIG. 6. Magnified SREM image of the Si (001) surface after vacancy introduction and thermal heating at 718 °C for 10 min. Preferential vacancy annihilation at the end of dimer rows causes retraction of the S_B steps and forms dark contrast 2×1 terraces underneath the S_B steps. The width of the denuded zone formed on the upper 1×2 terrace is wider than that of the lower side of the step band.

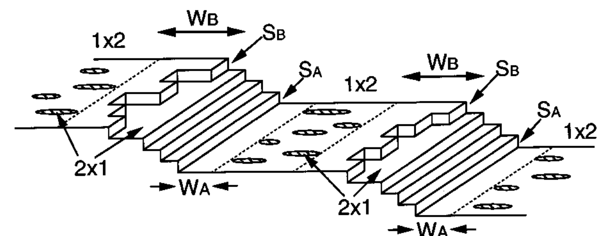

FIG. 7. Schematic illustration of denuded zone formation on the Si(001) surface. Preferential vacancy annihilation at the S_B steps results in wider denuded zones along the S_B steps. The diffusion length of vacancies along the dimer rows can be estimated from the width of the denuded zones.

With an increase of the annealing time and temperature, we confirmed that the vacancy islands grew laterally and moved away from the steps. In our previous report[19] we discussed possible processes that would explain these phenomena (Fig. 7 in Ref. 19). When we consider Si adatoms released from the steps of the vacancy islands or naturally existing steps, neither the motion nor the growth of vacancy islands would be allowed. Thus we introduced the anisotropic emission of vacancies outside of the vacancy islands. That is, when vacancies are annihilated at naturally existing step edges, a selective emission of vacancies takes place at the side of the step edges of vacancy islands neighboring initially existing step edges. This selective emission is driven by the density gradient of vacancies on terraces. To create vacancies, Si atoms at the step edges must move forward inside the vacancy islands. This results in vacancy island motion away from the naturally existing steps. Moreover, the growth of vacancy islands takes place due to the vacancy supply from neighboring islands and by the gathering together of vacancy islands. Therefore, the diffusion length of the vacancies can be evaluated from the denuded zone width.

After high-temperature annealing [Fig. 5(b)], denuded zones seem to be formed both along and perpendicular to the dimer rows on the wide 1×2 terraces. However, considering the preferential vacancy diffusion along the dimer rows, the creation of vertical denuded zones (perpendicular to the dimer rows) in these SREM images can be attributed to vacancy annihilation at wavy steps along the dimer rows. When the steps on the wide 1×2 terraces run horizontally (along dimer rows), formation of a denuded zone across the dimer rows can hardly be recognized, as indicated by the dotted arrow in Fig. 5(b). This means that the vacancy diffusion length along the dimer rows can be measured from these SREM images. Since thermal diffusion of vacancies is dominated by Brownian motion, the diffusion constant D is given by the relationship between annealing time t and diffusion length x as $D=x^2/t$. For example, the vacancy diffusion constant was calculated to be $(4.4\text{–}8.4)\times 10^{-12}$ $\mathrm{cm^2/s}$ at a 737 °C substrate temperature. This value is about five times larger than that of the vacancy diffusion on the Si(111) surfaces[19] and one order less than that of Si adatom diffusion along the dimer rows on the Si(001) surface.[23] (The difference in these diffusion constants also means that adatom diffusion does not play a major role in our SREM study.) The results indicate that vacancy diffusion on the Si(001) surface has an easier reaction path relating to the surface reconstruction, but the vacancies diffuse more slowly than adatoms. Figure 8 is an Arrhenius plot of the diffusion constant of vacancies determined from SREM images versus annealing temperature over the range from 597 °C to 737 °C. All experimental data fit well with the dotted line shown in this figure. The activation energy for vacancy diffusion was 2.3 ± 0.2 eV.

C. Model for vacancy diffusion on Si(001)

The activation energy obtained from the change in the denuded zone width is attributed to the potential barrier for vacancy diffusion on the terraces. Assuming the vacancy motion that occurs on a simple cubic isotropic surface, the Si atoms next to the vacancies must move in the opposite direction to the vacancy motion. So we describe the elemental process of vacancy diffusion on the terrace as being caused by the adatom release from steps and by adatom diffusion. Therefore, the diffusion constant D is given

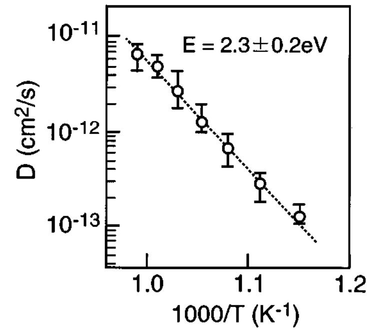

FIG. 8. Arrhenius plots for vacancy diffusion length in the temperature range from 597 °C to 737 °C. An activation energy of 2.3 ± 0.2 eV was obtained for vacancy diffusion along the dimer rows on Si(001) surfaces.

$$D=A\exp[-(E_s+E_b+E_{\mathrm{Sw}})/kT], \quad (1)$$

where A, E_s, E_b, E_{Sw}, and T are the frequency factor, the activation energy for surface diffusion of adatoms, the lateral binding energy of Si atoms at step edges, the Schwoebel barrier energy, and the substrate temperature. When we use the values of E_S and E_b reported for previous studies of homoepitaxial Si(111) surfaces ($E_s=1.3$ eV and $E_b=1.6$ eV) and the Schwoebel effect is negligible ($E_{\mathrm{Sw}}=0$ eV),[21,24,25] the experimentally obtained activation energy for the Si(111) surface (3.0 eV) is successfully explained ($E_s+E_b+E_{\mathrm{Sw}}=2.9$ eV).[19] If we apply this simple model to the Si(001) case, the small activation barrier of adatom diffusion along the dimer rows [$E_s=0.67$ eV (Ref. 2)] reduces the potential barrier for vacancy diffusion. As a primitive discussion, we can predict the activation energy for vacancy diffusion to be about 2.27 eV by using the energy value $E_b=1.6$ eV, even for Si(001) surfaces. This value is surprisingly close to our experimental results (2.3 ± 0.2 eV). However, we should also carefully consider the vacancy diffusion model for Si(001) surfaces based on the 2×1 reconstruction as follows.

STM images of clean Si(001) surfaces prepared by annealing always show that typical defects are not missing sites of individual atoms, but single-dimer vacancies (missing dimers) and their complexes.[1,9] Therefore, layer-by-layer sputtering at elevated substrate temperatures must be mediated by surface defects related to dimer vacancies. The activation energy obtained by Kitamura, Legally, and Webb by using STM was 1.7 ± 0.4 eV for single-dimer vacancy diffusion along the dimer rows at a sample temperature range between 217 °C and 252 °C.[15] This value is much smaller than that of our result and the theoretical estimation of dimer vacancy diffusion (2.5 eV) reported by Wang, Arias, and Joannopoulos, in which they calculated the potential barrier by assuming a sequence of simple bond breaking.[16] The most possible mechanism, which could reduce the activation barrier of single-dimer vacancy diffusion, is a coherent exchange of pairs of atoms between the top and the second

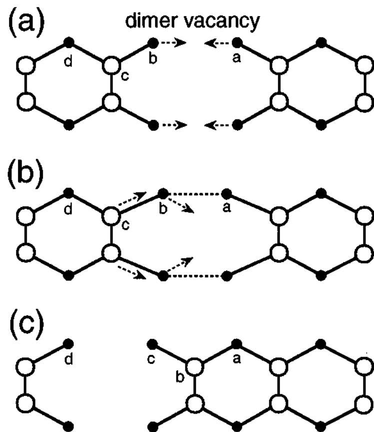

FIG. 9. Schematic illustration of the coherent exchange reaction, which allows diffusion of a single-dimer vacancy along the dimer row. The open and filled circles are top- and second-layer atoms, respectively. In this reaction, the second-layer atoms at the dimer vacancy are first brought together to form rebonding sites. Then a pair of second-layer atoms move up to form a neighboring ad-dimer and the connecting dimer is pulled down to the second layer.

layer (Fig. 9). In this reaction, the second-layer atoms at the dimer vacancy are first brought together to form rebonding sites [atoms a and b in Fig. 9(a)]. Then a pair of second-layer atoms moves up to form a neighboring ad-dimer [atoms b in Figs. 9(b) and 9(c)] and the connecting dimer is pulled down to the second layer [atoms c in Figs. 9(b) and 9(c)]. In the latest theoretical study, Yamasaki, Uda, and Terakura calculated the energy barrier for this coherent exchange reaction to be about 1.6 eV.[17] This correlates well with the STM experiment. These results mean that the diffusion process of a single-dimer vacancy does not govern the actual layer-by-layer sputtering process observed in our SREM experiment at a temperature range between 597 °C and 737 °C.

According to an *ab initio* total-energy calculation, some kinds of dimer vacancy complexes, such as a cluster of two-dimer vacancies and single-dimer vacancies neighboring a cluster of two-dimer vacancies, significantly reduce the surface energy.[16] The basic mechanism of reducing energy is the elimination of dangling bonds and the release of surface stress. The favorable configuration of dimer vacancy complexes consists of a pair of rebonded and nonrebonded second-layer atoms (Fig. 10). A recent detailed STM study

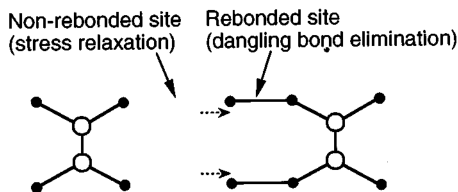

FIG. 10. Schematic illustration of the basic component of an energetically favorable dimer vacancy complex. This configuration is characterized by a pair of rebonded and nonrebonded second-layer atoms, which eliminates dangling bonds and releases surface stress.

showed the presence of this configuration on Si(001) surfaces after high-temperature annealing.[6] In our experimental conditions, although there must be an energy barrier for vacancy clustering, thermal annealing over 597 °C can form dimer vacancy complexes at the initial stage of thermal treatment. Since, in the basic component illustrated in Fig. 10, the center atoms of the second layer of the divacancy move toward either side of the defect, vacancy transport by the simple coherent exchange reaction shown in Fig. 9 cannot be expected at the nonbonded sites. When we assume an unstable configuration with two pairs of rebonded sites or dissociation of these vacancy complexes, there must be excess potential barrier for the surface diffusion of the vacancy complexes. Therefore, the excess activation energy obtained in our SREM experiment (2.3 ± 0.2 eV) compared to the case of a single-dimer vacancy (1.7 eV) can be attributed to the energy potential necessary to overcome an unstable configuration. This means that there are two vacancy diffusion temperature regions, which have different activation barriers depending on the cluster size. A similar discussion has also been made for homoepitaxial surfaces, as described in Eq. (1), where the activation energy estimated from the denuded zones of two-dimensional islands increases with an increase in substrate temperatures due to the change of critical nuclear size.[24,25]

Finally, we discuss possible mechanisms for selective vacancy annihilation at S_B steps. Swartzentruber and Schacht reported that fluctuations of S_B steps on Si(001) surfaces was frequently observed in STM images at temperatures over 230 °C.[14] The step rearrangement events were always comprised of multiples of four-atom units including two dimers and the effective activation energy barrier for step rearrangement was estimated to be 1.3 ± 0.3 eV. This suggests that dimer vacancy annihilation at steps should occur with a pair of dimer vacancies with lower activation barrier than the experimentally obtained value for dimer vacancy diffusion. When anisotropic dimer vacancy diffusion along the dimer rows on the 1×2 terraces transports vacancies to the lower and upper steps, vacancy complexes coming from upper terraces can be easily annihilated at lower S_B steps. However, vacancy diffusion toward the upper S_A steps results in the formation of local double atomic height steps. In this case, because a large-scale rearrangement is required to fill up the vacancy and because an unstable kink site is formed on the straight S_A step, vacancy annihilation on the S_A step should be much slower than on the S_B step. However, for a Si(111) surface, we could not observe any difference in vacancy annihilation rates between upper and lower terraces; that is, the Schwoebel effect was not recognized.[19] These results mean that the presence of dimers on Si(001) surfaces requires a much more complicated bond rearrangement for vacancy annihilation at S_A steps. However, a detailed explanation requires further investigation.

IV. CONCLUSION

We have investigated the kinetics of vacancy diffusion and annihilation on Si(001) surfaces by using SREM. Low-energy Ar-ion sputtering at elevated substrate temperatures results in layer-by-layer atom removal through a reversal of the step-flow mode or two-dimensional vacancy island

nucleation, depending on both the vacancy mobility and terrace width. The notable features for the Si(001) surface are anisotropic vacancy diffusion along the dimer rows and selective annihilation at the S_B steps. These processes form a single-domain-stabilized surface. From measurement of absolute step motion during ion sputtering, it was found that vacancy annihilation at S_B steps occurs 1.8 times faster than at S_A steps. By measuring the diffusion length from the width of the denuded zones, the activation energy for vacancy diffusion along the dimer rows was obtained to be 2.3 ± 0.2 eV at a temperature range between 597 °C and 737 °C. At these temperatures, the activation energy of vacancy diffusion increases from that of a single-dimer vacancy dominated at low substrate temperatures to that of vacancy diffusion mediated by stable dimer vacancy complexes.

ACKNOWLEDGMENTS

The authors are grateful to Dr. Takahiro Yamasaki of JRCAT for valuable comments on the vacancy diffusion model. This work, partly supported by NEDO, was performed at JRCAT under a joint research agreement between NAIR and ATP.

[1] R. M. Tromp, R. J. Hamers, and J. E. Demuth, Phys. Rev. Lett. **55**, 1303 (1985).
[2] Y.-W. Mo and M. G. Lagally, Surf. Sci. **248**, 313 (1991).
[3] Y.-W. Mo, J. Kleiner, M. B. Webb, and M. G. Lagally, Surf. Sci. **268**, 275 (1992).
[4] T. Tabata, T. Aruga, and Y. Murata, Surf. Sci. **179**, L63 (1987).
[5] R. A. Wolkow, Phys. Rev. Lett. **68**, 2636 (1992).
[6] F.-K. Men, A. R. Smith, K.-J. Chao, Z. Zhang, and C.-K. Shih, Phys. Rev. B **52**, R8650 (1995).
[7] J. D. Chadi, Phys. Rev. Lett. **59**, 1691 (1987).
[8] A. J. Hoeven, J. M. Lenssinck, D. Dijkkamp, E. J. van Loenen, and J. Dieleman, Phys. Rev. Lett. **63**, 1830 (1989).
[9] O. L. Alerhand, N. A. Becker, J. D. Joannopoulos, D. Vanderbilt, R. J. Hamers, and J. E. Demuth, Phys. Rev. Lett. **64**, 2406 (1990).
[10] P. Bedrossian, J. E. Houston, J. Y. Tsao, E. Chason, and S. T. Picraux, Phys. Rev. Lett. **67**, 124 (1991).
[11] E. Chason, P. Bedrossian, J. E. Houston, J. Y. Tsao, B. W. Dodson, and S. T. Picraux, Appl. Phys. Lett. **59**, 3533 (1991).
[12] P. Bedrossian and T. Klitsner, Phys. Rev. Lett. **68**, 646 (1992).
[13] B. S. Swartzentruber, C. M. Matzke, D. L. Kendall, and J. E. Houston, Surf. Sci. **329**, 83 (1995).
[14] B. S. Swartzentruber and M. Schacht, Surf. Sci. **322**, 83 (1995).
[15] N. Kitamura, M. G. Lagally, and M. B. Webb, Phys. Rev. Lett. **71**, 2082 (1993).
[16] J. Wang, T. A. Arias, and J. D. Joannopoulos, Phys. Rev. B **47**, 10 497 (1993).
[17] T. Yamasaki, T. Uda, and K. Terakura, Phys. Rev. Lett. **76**, 2949 (1996).
[18] H. Watanabe and M. Ichikawa, Appl. Phys. Lett. **68**, 2514 (1996).
[19] H. Watanabe and M. Ichikawa, Phys. Rev. B **54**, 5574 (1996).
[20] H. Watanabe and M. Ichikawa, Rev. Sci. Instrum. **67**, 4185 (1996).
[21] M. Ichikawa and T. Doi, in *Reflection High Energy Electron Diffraction and Reflection Electron Imaging of Surfaces,* Vol. 188 of *NATO Advanced Study Institute, Series B: Physics*, edited by P. K. Larsen and P. J. Dobson (Plenum, New York, 1988), p. 343.
[22] A. V. Latyshev, A. B. Krashilnikov, A. L. Aseev, and S. I. Stenin, Pis'ma Zh. Eksp. Teor. Fiz. **48**, 484 (1988) [JETP Lett. **48**, 526 (1988)].
[23] T. Doi, M. Ichikawa, S. Hosoki, and K. Ninomiya, Surf. Sci. **343**, 24 (1995).
[24] A. V. Latyshev, A. B. Krashilnikov, and A. L. Aseev, Phys. Status Solidi A **146**, 251 (1994).
[25] H. Nakahara, M. Ichikawa, and S. Stoyanov, Surf. Sci. **329**, 115 (1995).